The conventional dimerization constant for $2C_2H_5COOH \rightleftarrows (C_2H_5COOH)_2$ was given by

$$K_D = \frac{C_D}{(C - C_D)^2} = \frac{x_D}{2C(1 - x_D)^2} \quad (43)$$

where C is the total acid concentration, and C_D ($=x_DC/2$) is the concentration of acid dimer. Note that our discussion outlined above is also valid when we use a simple "intensity ratio" $[H^+C_2H_5COOH(H_2O)_{n-1}]/[H^+(H_2O)_n]$ instead of the population ratio (left hand side of eq 4) that was derived by calibrating electron impact ionization cross section, mass dependence of the mass spectrometer, and the cluster size distribution of the beams.

Table VII presents a compilation of the result with some dimerization constants in solutions as well as those in the gas phase. The present K_D value obtained from the cluster distribution is close to the values obtained by other measurements such as potentiometric titration of bulk aqueous solution. The small difference between our result of log $K_D = -0.4$ and the other results of log ${}^TK_D = -0.64$ to -1.01 (line numbers 3 and 4 in Table VII) may be explained mainly by the difference of the definition of the dimerization constant. ${}^TK_D$ were defined by the activities of the solutes (${}^TK_D = [a(A_2)]/[a(A)]^2$) where $a(A_2)$ and $a(A)$ are the activities of solute dimer and solute monomer, respectively. The slight difference between our result (log $K_D = -0.4$) and the value from Carson and Rossotti[7] (log $K_D = -0.50$) may be explained by the difference of the solution temperatures (55 °C and 25 °C). Temperature dependence of K_D for propionic acid is expected to be small and positive for the temperature increase because the enthalpy of dimerization (ΔH_D) in H_2O is 0.4 kcal/mol for acetic acid.[38] The dimerization constant in the gas phase[40] is more than 10^4 greater than those in aqueous solution.[7] The coincidence of dimerization constants of propionic acid both in bulk solution and in the isolated clusters confirmed that *the compositions of the clusters separated from aqueous solutions reflect the association properties in the original solutions.*

Registry No. HCOOH, 64-18-6; CH_3COOH, 64-19-7; C_2H_5COOH, 79-09-4; C_3H_7COOH, 107-92-6; C_4H_9COOH, 109-52-4; $C_5H_{11}COOH$, 142-62-1; H_2O, 7732-18-5.

(40) Taylor, M. D.; Bruton, J. *J. Am. Chem. Soc.* **1952**, *74*, 4151.

Fundamental Studies of Microscopic Wetting on Organic Surfaces. 1. Formation and Structural Characterization of a Self-Consistent Series of Polyfunctional Organic Monolayers

Ralph G. Nuzzo,*,† Lawrence H. Dubois,*,† and David L. Allara*,‡

Contribution from the AT&T Bell Laboratories, Murray Hill, New Jersey 07974, and Departments of Chemistry and Materials Science and Engineering, Pennsylvania State University, University Park, Pennsylvania 16802. *Received February 17, 1989*

Abstract: Monolayers of a series of terminally substituted alkyl thiols, $X(CH_2)_{15}SH$ (X = CH_3, CH_2OH, CO_2H, CO_2CH_3, and $CONH_2$), have been prepared by adsorption from solution onto evaporated gold substrates. The structures have been characterized by infrared (IR) spectroscopy, X-ray photoelectron spectroscopy (XPS), ellipsometry, and temperature-programmed desorption (TPD). The IR data shows the monolayer films to be densely packed, crystalline-like structures with all-trans conformation alkyl chains exhibiting average tilt angles of the chain axis in a range of 28–40° from the surface normal and an approximate 55° twist of the chain axis away from a configuration with the CCC plane perpendicular to the surface plane. TPD results set a lower limit of interaction between the CH_2 groups in the films of ~0.8 kcal/mol. We find that the terminal groups are exposed at the ambient interface, and, based on an analysis of the IR data, an assessment of the conformations and molecular environments of these groups is made. The CO_2H terminal groups appear to exist in short hydrogen-bonded (perhaps dimeric) sequences. Detailed examination of the IR data shows some unexplained abnormalities with respect to the quantitative treatment of the terminal functional group spectra. These effects can be traced to the perturbations which occur when a group is placed at an interface relative to the environment experienced in a crystalline solid. The major feature of this study is the finding that the reported series of derivatives form a structurally self-consistent set of well-defined reagent surfaces suitable for use in further studies of the surface properties of organic materials.

The chemisorption of organosulfur compounds on gold surfaces has proven to be a remarkably useful and powerful synthetic methodology for the construction of well-defined organic surfaces and interfaces.[1-9] Recent papers have established the general characteristics of the surface phases obtained with several structurally diverse adsorbate systems, in particular simple aliphatic and certain substituted disulfides,[1,3,4] the *n*-alkyl thiols,[5,10] and a broad range of symmetrical and unsymmetrical dialkylsulfides.[2] Diffraction studies have also demonstrated ordering in certain phases formed from long-chain *n*-alkyl thiols.[11] Whitesides and co-workers have detailed structural relationships in wetting behavior by using this chemisorption system.[2,5-7,9] Similar relationships were also established in UHV chemisorption studies by Dubois et al.[12] The combined weight of this reported work establishes several important general principles. First, when

Scheme I

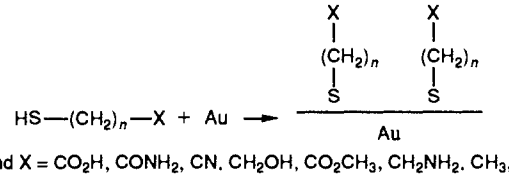

($n \geq 1$ and X = CO_2H, $CONH_2$, CN, CH_2OH, CO_2CH_3, CH_2NH_2, CH_3, $CHCH_2$, etc.)

† AT&T Bell Laboratories.
‡ Pennsylvania State University.

(1) Nuzzo, R. G.; Allara, D. L. *J. Am. Chem. Soc.* **1983**, *105*, 4481–83.
(2) Troughton, E. B.; Bain, C. D.; Whitesides, G. M.; Nuzzo, R. G.; Allara, D. L.; Porter, M. D. *Langmuir* **1988**, *4*, 365–385.

0002-7863/90/1512-558$02.50/0 © 1990 American Chemical Society

suitably selected, these adsorbates self-assemble on the gold surface to form coherent, densely packed monolayer films. Second, the monolayers formed are very stable and suitable for application in a broad range of physical and chemical studies.

Several recent papers, and others soon to appear, are concerned with the microscopic origins of such complex properties as wetting (contact angle behavior), adhesion, interfacial reactivity, electron-transfer kinetics, and molecular adsorption. What has become the standard synthetic protocol in these studies is the adsorption from solution of various *n*-alkyl thiols (and substituted analogues) on nominally clean gold surfaces as illustrated qualitatively in Scheme I. Although certain aspects of the nature of these films can be inferred from the data already available in the literature, a detailed examination of the structural variations exhibited by a self-consistent series involving only simple substitutions of the functionality X has not been presented. It must be emphasized that any such sensitivity or variation of the film structure is of overwhelming concern to the types of studies described above.

The structural questions of interest in this study are also fundamentally related to the larger need of developing a better understanding of the microscopic origins of structure in low-dimensional organic phases. For example, if, as we expect, the surface phases formed by these absorbates on gold consist of canted (i.e., tilted) chains in a closest packed monolayer,[4,10] one can ask whether variation of the X group produces significantly different molecular orientations. Is conformational disordering induced by such substitutions an important process? It is also easy to envision how such effects could arise as a result of the strong, directional characteristics of hydrogen bonding and dipolar interactions, features characterizing several of the adsorbates examined in this study. One can also ask does the surface coverage remain constant throughout a given series of chain substitutions. How questions such as these are related to the issue of physical properties can be demonstrated easily by consideration of the specific example of contact angle (wetting) behavior. It is clear that a necessary outcome of film disorder is the presentation of a compositionally more complex phase at the wetted interface. For adsorbates containing polar substituents, the properties of the surface phase formed thus may reflect not only the contributions of that group but the underlying aliphatic spacer as well. Such disordering as well as more complex phase transitions involving changes in molecular orientation also can increase effectively the spatial separation of the chain termina in two dimensions, thus imposing an additional experimental complication unrelated to simple substitutions of groups. High packing densities and preferred orientations of functional groups at the ambient interface might also give rise to steric screening effects (in which access to a portion of a functional group is blocked physically), which need to be considered when one explores how external phases interact with these and other model organic solids.[7,9,12]

The present paper reports a study of the effects on structure of varying the nature of the chain-terminating functionality in a structurally self-consistent series of *n*-alkyl thiol monolayers on gold (Scheme I). We have chosen for convenience a chain length of $n = 15$ and constituent functionality of X = CH_3, CH_2OH, CO_2H, $CONH_2$, and CO_2CH_3. Earlier studies[5,10] have shown that hydrocarbon chains of these lengths (or longer) give high quality monolayers as evidenced by such measures as ellipsometry, X-ray photoelectron spectroscopy (XPS), infrared (IR) spectroscopy, electrochemical properties, and contact angle behavior. The variety of X groups examined represents, as well, a range of chemically distinct functionalities with properties of interest to wetting and reactivity studies. As we will show, these monolayers are highly oriented and, quite likely, ordered. Our evidence strongly supports both consistent surface coverage with high packing density and a constant average alkyl chain orientation for all the monolayers studied. These films thus provide a uniform set of material structures which differ primarily in the nature of the exposed functionality at the ambient surface. These features will be used as a basis for developing an understanding of the complex behaviors of organic surface phenomena which are currently under investigation.[12]

Experimental Section

General Methods. Many of the details involved in similar experiments have been reported elsewhere. For the benefit of the reader a qualitative discussion is provided and specific references cited. Samples were prepared by e-beam evaporation of >2000 Å of gold onto clean, polished silicon single-crystal wafers which had been primed with an adhesion layer of ~40 Å of titanium. The base operating pressure of this cryopumped evaporator is $\sim 5 \times 10^{-9}$ Torr. The sample was not allowed to rise above ~40 °C during the evaporation. Previous studies[4] have established that this procedure produces polycrystalline gold films exhibiting a strong (111) texture and grains >1000 Å in size. The sample properties are thus dominated by the phases which self-assemble on large, flat (111) terraces. Samples were immersed in ethanol solutions of the adsorbate ($\sim 10^{-3}$ M) contained in glass jars. No precautions were taken to exclude air. Monolayer samples on Au(111) single-crystal surfaces were prepared as described in the following paper in this series.[12b] Ellipsometry measurements were made with a Gaertner Model L-116B ellipsometer, with 6328 Å radiation (HeNe laser) at a 70° angle of incidence. The details of the analysis have been described elsewhere.[13] XPS data were obtained with a Kratos XSAM 800 photoelectron spectrometer operating in the fixed analyzer transmission mode. We have observed that these materials are extremely sensitive to the X-ray source (presumably a decomposition due to the secondary electron emission), and, as a result, the X-ray flux was kept as low as signal-to-noise constraints would allow. The decomposition we observe complicates a quantitative interpretation of the XPS data (especially the line shapes) but in general is qualitatively predictive of the type of surface phase formed.

Infrared Spectroscopy. IR data were obtained with a Digilab Model 15-80 spectrometer with custom optics optimized for grazing incidence reflection. The effective limiting frequency range in this instrument is 800–4000 cm^{-1}. Analysis of the infrared data was done according to the protocol described in detail in earlier publications.[4,13]

The salient feature of this or other equivalent approaches is the treatment of the absorption spectra in terms of quantities intrinsic to the state of the material and not specific to the manner in which the spectra were taken. The appropriate intrinsic quantity is the frequency dependent complex optical function, $\hat{n}$, defined as

$$\hat{n} = n + ik = \hat{\epsilon}^{1/2} \tag{1}$$

where n and k are the real and imaginary parts of the function, respectively, and $\hat{\epsilon}$ is the dielectric function of the material.[14] Normally absorption spectra are treated solely in terms of k, the absorption coefficient, but for many experimental configurations (e.g., reflection and diffuse scattering) n has a very pronounced effect on the observed spectra. Quantitation requires the rigorous consideration of these effects. Our approach has involved the experimental determination of $\hat{n}$ for a convenient reference state, usually a polycrystalline dispersion in a KBr matrix, and comparison of the observed glancing angle reflection spectrum with a transformed polycrystalline spectrum where account has been made for the effects of n on the reflection spectrum. This transformed spectrum is essentially that of a thin isotropic layer of polycrystalline compound on a planar gold substrate excited under the experimental conditions of the actual observed spectrum. The intensity of

(3) Nuzzo, R. G.; Zegarski, B. R.; Dubois, L. H. *J. Am. Chem. Soc.* **1987**, *109*, 733–40.
(4) Nuzzo, R. G.; Fusco, F. A.; Allara, D. L. *J. Am. Chem. Soc.* **1987**, *109*, 2358–2368.
(5) Bain, C. D.; Troughton, E. B.; Tao, Y.-T.; Evall, J.; Whitesides, G. M.; Nuzzo, R. G. *J. Am. Chem. Soc.* **1989**, *111*, 321–335 and references cited therein.
(6) Bain, C. D.; Whitesides, G. M. *J. Am. Chem. Soc.* **1988**, *110*, 6560–1.
(7) Bain, C. D.; Whitesides, G. M. *J. Am. Chem. Soc.* **1988**, *110*, 5897–8.
(8) Diem, T.; Czajka, B.; Weber, B.; Regen, S. L. *J. Am. Chem. Soc.* **1986**, *108*, 6094–5.
(9) Bain, C. D.; Whitesides, G. M. *Science (Washington, D.C.)* **1988**, *240*, 62–3.
(10) Porter, M. D.; Bright, T. B.; Allara, D. L.; Chidsey, C. E. D. *J. Am. Chem. Soc.* **1987**, *109*, 3559–68.
(11) (a) Electron diffraction. Strong, L.; Whitesides, G. M. *Langmuir* **1988**, *4*, 546–558. (b) Helium diffraction: Chidsey, C. E. D.; Liu, G.-Y.; Rowntree, P.; Scoles, G. *J. Chem. Phys.* **1989**, *91*, 4421–4423.
(12) (a) Dubois, L. H.; Zegarski, B. R.; Nuzzo, R. G. *Proc. Natl. Acad. Sci. U.S.A.* **1987**, *84*, 4739–42. (b) Dubois, L. H.; Zegarski, B. R.; Nuzzo, R. G. *J. Am. Chem. Soc.*, following paper in this issue.
(13) Allara, D. L.; Nuzzo, R. G. *Langmuir* **1985**, *1*, 52–66.
(14) Jackson, J. D. *Classical Electrodynamics*, 2nd ed.; J. Wiley: New York, 1975.

Table I. Spectral Mode Assignments and Calculated Transition Moment Directions for *n*-Hexadecanethiol on Au

freq, cm^{-1}				
obs	calc[b]	mode assignment[a]	$I_{obs}/3I_{calc}$	θ_{mz}, deg
2965	2962 (sh)	CH_3 C–H str (asym, ip), r_a^-	0.82	25
~2958 (sh)	2955	CH_3 C–H str (asym, op), r_b^-	~0.13	~69
2938	~2943	CH_3 C–H str (sym, FR)[c]	≳0.5	45
2919	2920	CH_2 C–H str (asym), d^-	0.24	61
2878	2872	CH_3 C–H str (sym, FR)[c]	~1.4	
2851	2850	CH_2 C–H str (sym), d^+	0.18	65
1468	1471	CH_2 scissors def, δ_{CH_2}	0.16	66
1383	1372	CH_3 def (sym) δ_{CH_3}		
~1150–1350	~1150–1350	chain wags and twists[d]	*e*	39[e]

[a] Mode assignment nomenclature: str = stretch, asym = antisymmetric, sym = symmetric, ip = in-plane, FR = Fermi resonance, def = deformation. Literature sources for the assignments are given in ref 4, 10, and 13. [b] Details given in text. [c] Band is split by Fermi resonance interactions with lower frequency CH_3 deformation mode. [d] The larger bands in the calculated spectrum appear at 1185, 1203, 1225, 1247, 1270, 1292, and 1312 cm^{-1}. The experimental spectrum exhibits weak peak-like features at ~1183, 1205, 1223, 1244, 1263, 1282, 1306, 1326, and 1349 cm^{-1}. The absorptions on this region are actually comprised of a wagging series and a twisting series. The normal mode description of the latter involves a combination of twisting and rocking motions (see ref 20). [e] The poor signal-to-noise characteristics of the wag-twist series bands in the experimental spectrum makes calculation of the θ_{mz} values tenuous. However, choosing the two strongest pairs of observed and calculated bands (1183, 1185 and 1223, 1225 cm^{-1}), we calculate θ_{mz} values of ~34 and 44° for an average of ~39°. On the basis that the modes derive from a $(CH_2)_{15}$ polymethylene chain, these bands were assigned as members of the wagging series with values of 1 and 3 for the integers describing the specific eigenstate (see ref 20 and 22). The odd integer members should be the most intense of the chain modes and are associated with transition moments parallel to the chain axis (ref 22).

the transformed spectrum depends, in part, upon the layer thickness, and, in this paper, measured ellipsometric thicknesses were used (see below). Comparisons of the calculated and observed spectra, thus, should be free of optical dispersion effects within the bounds of treating $\hat{n}$ (or $\hat{\epsilon}$) as a scalar[15] and reflect intrinsic structural differences between the monolayer and the bulk solid. For these types of monolayer structures, our experience has shown that differences in line shapes and peak frequencies are usually indicative of differences in intra- and intermolecular packing, while intensity differences are usually indicative of monolayer coverage and structural anisotropy, although more subtle effects of electron density redistribution caused by changes in molecular interactions are possible.

The reference state used for the determination of optical constants was, with one exception, the bulk solid in a KBr dispersion. Hexadecanethiol, which is a liquid, could not be done in this manner. As a result of this, calculations were performed with optical constants derived from di-*n*-hexadecyldisulfide,[4] a material which should quite reasonably predict the spectral properties of an *n*-hexadecyl chain bonded to a divalent sulfur atom.

Materials. Absolute ethanol (USI), the solvent used for all sample incubations, was used as received. Gold (>99.999%) and titanium (>99.95%) were obtained from Alpha. Hexadecanethiol was obtained from Aldrich and passed through a plug of Woehlem Activity-1 alumina before use. The thiols 16-mercaptohexadecanoic acid, methyl 16-mercaptohexadecanoate, and 16-mercapto-1-hexadecanol were prepared according to procedures which have been described elsewhere.[5]

16-Mercaptohexadecanamide. This material was prepared according to a minor modification of a procedure reported in the literature for the synthesis of 16-mercaptohexadecanoic acid[5] in which 16-bromohexadecanamide is substituted for 16-bromohexadecanoic acid. The bromoamide was prepared from the corresponding acid by first converting it to the acid chloride with oxalyl chloride according to standard procedures. The crude acid chloride (~3.0 g) was dissolved in 25 mL of methylene chloride and added in a stream to 200 mL of a vigorously stirred, 50:50 (V) solution of H_2O and NH_4OH. The amide was collected by filtration, dried, and recrystallized twice from ethanol (mp 114–115 °C).

Results and Discussion

General Observations. Immersion of a gold film into an ethanol solution of any of the thiols described in this study results in the formation of a self-assembled monolayer film. Incubation times of ~1 day typically were used, although on occasion longer immersions in the adsorbate solutions were employed. Earlier studies have shown that complex kinetics can characterize monolayer formation, and, as a result, we prefer to adopt overly long times to help insure equilibration.[16] Ellipsometric examination of the various monolayers yielded several interesting observations. First, the *intrinsic* thicknesses of the films formed by most of the adsorbates are all very similar. The values we measure are typically scattered in a small range about 22 Å, a value similar to, but slightly larger than, that found in a companion study.[5] Second, the thickest films generally were obtained from methyl 16-mercaptohexadecanoate (the values for this derivative were scattered about 24 Å), as might be expected from the addition of an extra carbon atom to the adsorbate chain. Third, the polar derivatives (16-mercaptohexadecanoic acid, 16-mercapto-1-hexadecanol, and 16-mercaptohexadecanamide) showed some tendency toward environmental contamination. This effect was especially pronounced on humid days and presumably reflects, in part, the adsorption of water from the air. Even so, it is possible to measure what we describe as being intrinsic film thicknesses with the simple expedient of rinsing the films with water (or ethanol) and measuring the samples under a nitrogen purge.

XPS Measurements. Examination of the films described above by X-ray photoelectron spectroscopy confirms that the monolayer surface phases formed reflect the adsorbates intended and not contaminants from air exposure or some adventitious (low volatility) impurity in the solution. Figure 1 shows a series of high-resolution core level spectra in the O1s and C1s regions for the various monolayers studied. Several significant features are apparent in the data. First, oxygen signals are only seen in the films formed from the adsorbates containing that atom (and, although not shown, the N1s core level is seen only in the amide). Second, the line shapes and obvious peak multiplicities in both the C1s and O1s regions are consistent in a qualitative manner with the functional groups present in the molecule.[17] We have not attempted a quantitative fit of this data as extensive decomposition was noted in our spectrometer even during brief acquisitions. We also note that qualitative angular dependent measurements are consistent with a sharp placement of the chain-terminating functionality at the monolayer-vacuum interface. These data are entirely consistent with that presented in detail elsewhere[5] and serve to confirm the identity of the materials whose structure is explored below by use of quantitative infrared spectroscopy.

Investigation of Film Structure, Bonding, and Molecular Orientation by Infrared Spectroscopy. Spectral peak frequencies along with mode assignments are presented in Tables I–V, and the spectra are shown in Figures 2–11. The assignments of the alkyl modes have been discussed previously, and the reader is referred to these sources where a number of detailed studies are cited.[1,4,10,13]

(A) Hexadecanethiol. We will discuss first the spectrum of a monolayer of adsorbed hexadecanethiol in detail. Although a

(15) Hayes, W.; Lowdon, R. *Scattering of Light by Crystals*; J. Wiley: New York, 1978.

(16) Allara, D. L.; Nuzzo, R. G. *Langmuir* **1985**, *1*, 45–52.

(17) The line shapes in the O1s core level region show poorly resolved, overlapping gaussian components for those derivatives containing oxygen atoms in two discrete bonding environments and single peaks in the rest (except the all-alkyl chain). Suitable assymetries are also evidenced in the C1s region. See the primary citation in ref 5 for a detailed discussion.

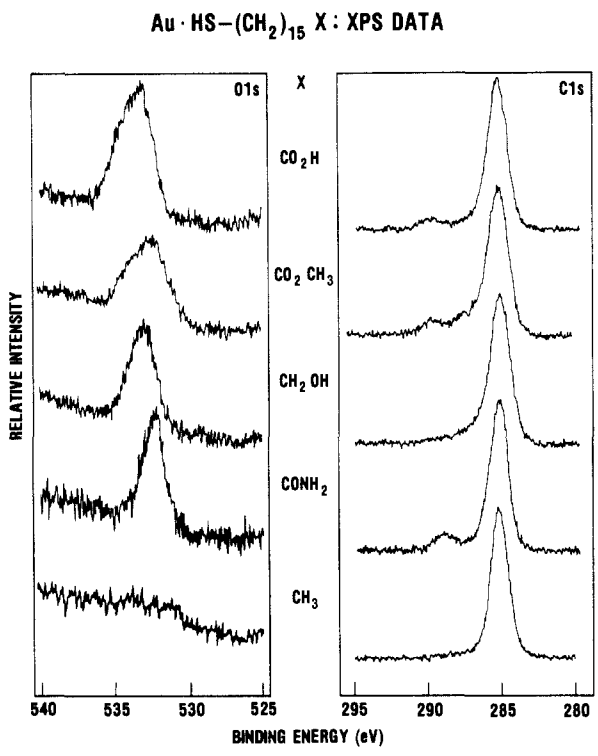

Figure 1. High-resolution XPS data showing the O1s and C1s core levels for a series of *n*-alkanethiols chemisorbed on gold.

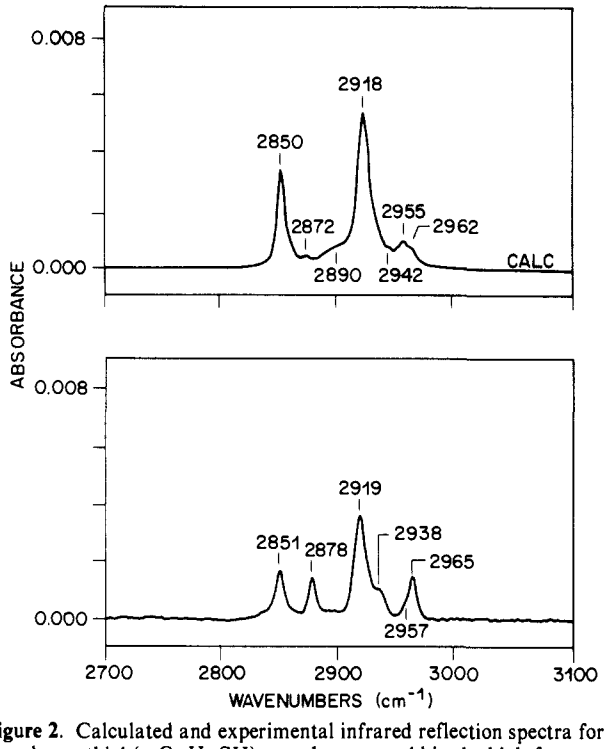

Figure 2. Calculated and experimental infrared reflection spectra for a hexadecanethiol (n-$C_{16}H_{33}SH$) monolayer on gold in the high-frequency region. The methods of calculation and analysis are described in the text.

previous paper[10] has dealt with certain structural aspects of this monolayer, it is useful to incorporate these results into our present discussion given the similarity of this long chain adsorbate to the functionalized adsorbates of interest herein. Since this previous study reported an estimate of the average chain orientation for the monolayer assembly but not a rigorous calculation, we report these details along with a better value here. The spectrum in the C–H stretching region is shown in Figure 2, and the mode assignments are given in Table I. Figure 2 also shows the monolayer spectrum calculated by transformation of the bulk crystallite KBr matrix spectrum (derived from di-*n*-hexadecyldisulfide, see above).

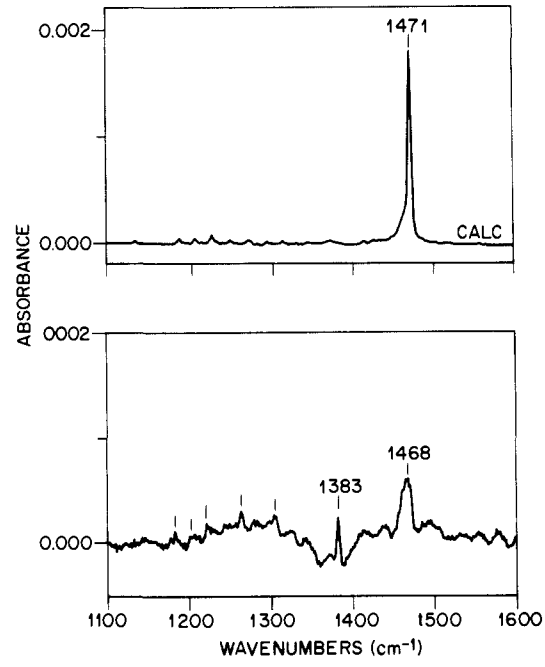

Figure 3. Data as in Figure 2 in the low frequency region.

The important features of these data are the positions of the d^- and d^+ CH_2 C–H stretching modes at 2919 and 2851 cm^{-1}, respectively, which we interpret as being indicative of crystalline-like packing of the alkyl chains. This reasoning in turn strongly implies all-trans conformational sequences since the presence of gauche defects is not consistent with high packing densities. A comparison of the calculated and observed line shapes also shows negligible differences, further indicating that a similar distribution of intermolecular environments exists for the CH_2 groups in both the crystalline bulk and the monolayer phases. The spectrum of the lower frequency region down to 1100 cm^{-1} (only increasing noise was observed down to the detector cut off at ~800 cm^{-1}) is given in Figure 3. The relative weakness of the 1468-cm^{-1} absorption, which we attribute to the CH_2 scissiors deformation, is consistent with a tilted orientation of the chain on the surface (see below). The narrow line width is consistent as well with a crystalline-like environment. Another observable feature in Figure 3 is the sharp peak at 1383 cm^{-1} (this mode resides in a weak negative baseline dip which is an artifact of the particular reference used). We assign this mode as the CH_3 symmetric deformation,[18,19] and note two peculiarities in regards to its character. First, it exhibits a considerable shift as compared to the bulk (1372 cm^{-1} in the reference state). Second, the intensity of the experimental band is extraordinarily large compared to the calculated value (the absorption in the calculated spectrum is not easily seen without a scale expansion). Both of these observations suggest that a significant perturbation of the methyl group exists in the monolayer, a point we will return to later in the manuscript.

Very weak features were observed in the calculated reference spectrum between ~1150 and 1350 cm^{-1} (Figure 3 and Table I). The majority of these are assigned straightforwardly to the CH_2 twisting and wagging modes which arise when an all-trans conformational sequence exists along the chain backbone such that coupling and dispersion of the modes can take place.[20] Similar weak features are seen in the experimental monolayer spectrum (Figure 3) as well, suggesting the presence of similar sequences. The noise levels are such, however, that a definitive assignment cannot be made.

(18) Schachtschneider, J. H.; Snyder, R. G. *Spectrochim. Acta* **1963**, *19*, 117–68.
(19) Bellamy, L. J. *The Infrared Spectra of Complex Molecules*; J. Wiley: New York, 1975.
(20) Snyder, R. G.; Schachtschneider, J. H. *Spectrochim. Acta* **1963**, *19*, 85–116.

Values of the average angles, θ_{mz}, between the transition dipole moments (m) and the surface normal (z) were calculated for various bands including the d^-, d^+, and δ modes of the CH_2 groups in the hexadecanethiol monolayer by using the calculated and observed absorption intensities in Figures 2 and 3. Details of the method of calculation are given elsewhere.[4,13] The protocol is based largely on the dependence of the absorption intensity on the scalar product of the surface electric field amplitude and the oscillator transition dipole moment. This gives rise on metallic substrates to the familiar relationship

$$I \propto \cos^2 \theta_{mz} \tag{2}$$

where I is the spectral intensity and θ_{mz} is defined above. The average orientation is then determined from the calculated reference spectrum, which represents an isotropic collection of the same molecules in similar packing densities, by using the relationship

$$\cos \theta_{mz} = (I_{obs}/3I_{calc})^{1/2} \tag{3}$$

where I_{obs} and I_{calc} are the observed and calculated spectral intensities. For a given chain orientation, one can relate the transition moment directions in surface coordinates to molecular coordinates by straightforward linear transformations.[13] On this basis, by using the transition moment directions in molecular coordinates in Table VI, an arrangement of an all-trans chain was determined which gave the best fit to the spectrally derived data in Table I.

As is shown in Table VII, the best fit is obtained for an *average* chain with a tilt angle, α, of 40° and a twist angle, β, of 50°, where α and β are as defined in Figure 12. This structure is in good agreement with the data of Strong and Whitesides[11a] which suggested a chain tilt of 25–35° in a similar alkanethiol monolayer on Au(111).[21] This result is also in good agreement with that previously obtained for a di-*n*-hexadecyldisulfide monolayer (α = 37°, β = 55°).[4]

A corresponding analysis of the C–H stretching modes for the methyl group (Figure 2 and Table I) proves to be problematic (see below): the value of $I_{obs}/3I_{calc}$ for the CH_3 C–H symmetric stretching mode absorption at 2879 cm^{-1} is 1.4 (our experimental error is estimated to be ~±0.1 here). Since, by eq 3, this quantity equals $\cos^2 \theta_{mz}$, an upper limit of 1 is imposed, and the observation of 1.4 implies that some assumption inherent in the interpretation of the data is incorrect. This problem may arise *in part* because of the strong influence of Fermi resonance on modes associated with the CH_3 group. This point will be discussed in more detail later when we specifically consider the spectral perturbations associated with the placement of a functional group at an ambient interface.

As the discussion above illustrates, an assignment of the main chain orientation can be made with a fair degree of confidence from an analysis of the C–H stretching modes associated with the methylene groups. This analysis, due to the symmetry of the chain, does not determine the sign of the chain cant angle, α (see Figure 12). This issue is not one of passing interest for the sign of α is crucial for defining the structure of the methyl surface phase and the divalent sulfur bond angles which are necessary to accommodate the bonding of the all-trans chain to the Au lattice plane. This aspect of structure is explicitly addressed by defining the molecular orientation of the chain termina. As has been noted above, the quantitative analysis of orientation fails for the various modes associated with the methyl group, suggesting an important contribution to the observed spectra from factors other than orientation. As a result, reliable orientations cannot be obtained for the methyl group from comparisons of observed spectra with transformed isotropic bulk phase spectra (the method implied in eq 3). It is possible, however, to define the sign of the tilt angle by making relative comparisons between observed monolayer spectra of alkanethiols with odd and even length carbon chains. Chart I shows approximate side projections for the last four carbon atoms in model hexadecanethiol monolayers where we have used the orientations predicted by the analysis of CH_2 modes above and let α vary in sign.

Chart I

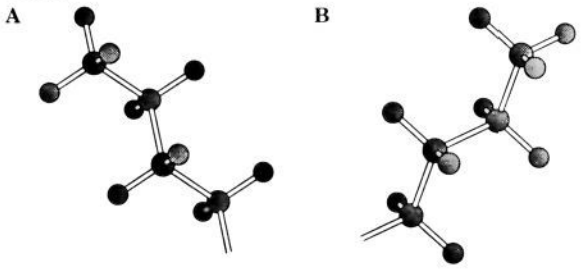

Notice that, were the chain length to increase by one carbon atom—that is *from an even to an odd chain length*—very different spectral patterns would emerge. In canted structures of this sort (where the expected changes in direction of the transition dipole moments of the CH_3 stretching modes relative to the surface normal will be significant in an odd–even series) large diagnostic changes in intensity should be observed. These intensity differences should also be of such a size and direction so as to easily distinguish them from the spectral perturbations noted above. The types of intensity changes expected can be seen easily from the directions of the transition moments for the CH_3 group given in Table VI. Specifically, we expect that, relative to structure A, the symmetric CH stretch (r^+) will be stronger for structure B, whereas the in-plane asymmetric stretch (r_a^-) will be weaker.

An example of the data obtained is shown in Figure 13 where infrared spectra in the high frequency region are shown for two monolayers: the heptadecane- and octadecanethiol monolayers on gold. When viewed together with the data shown in Figure 2, an obvious pattern emerges (a pattern we have demonstrated in control experiments in both the high and low frequency regions down to chain lengths as short as four carbon atoms). The obvious qualitative features of this particular data set are the intense asymmetric (2957, 2965 cm^{-1}) and weak symmetric (2878 cm^{-1}) methyl C–H stretches in the even CH_2 chain spectra and the very nearly equal intensities in the odd. These observations can be rationalized only for an odd CH_2 chain which gives rise to surface projection B in Chart I and an even CH_2 chain which switches to structure A. This analysis fixes the sign of the cant angle for the case of hexadecanethiol and orients the C–S bond in the general direction shown by the sketch in Figure 12. It is also interesting to note that this orientation would require the least severe perturbation of a typical divalent sulfur bond angle (~110°) to accommodate the chain packing.

(B) Substituted Alkanethiols: High-Frequency Modes. The terminally substituted alkanethiols show a number of significant structural features when their spectra are subjected to an analysis of orientation using eq 3. The results for the methyl ester, carboxylic acid, amide, and alcohol surfaces are presented in Figures 4–11, respectively. For each derivative we present calculated and measured spectra in both the high (~2500–3500 cm^{-1}) and low (~1000–2000 cm^{-1}) frequency regions of the spectrum.

Inspection of the data in the high frequency region (Figures 4, 6, 8, and 10) reveals that all the derivatives exhibit spectra with characteristics similar to the spectrum of hexadecanethiol. The d^+ and d^- absorptions are sharp and centered at ~2850 and ~2918 cm^{-1}, respectively (exact values are listed in Tables II–VI). These values strongly support the argument that these alkyl chains experience densely packed, crystalline-like environments quite similar to those found for the unsubstituted long chain thiol assemblies. Using eq 3, values of the transition moment directions were calculated for the d^+ and d^- modes for each derivative; the results are given in Tables II–V. By using the molecular coordinates given in Table VI, the chain orientations (in surface coordinates) were calculated and are presented in Table VII. The average value of the tilts (α) for all the chains is ~34° with a

(21) It is likely, although difficult to prove precisely, that the systematic errors in the IR analysis tend to overestimate the deduced cant angles. Were it possible to take proper account of these errors, an even closer agreement with the diffraction data would be obtained.

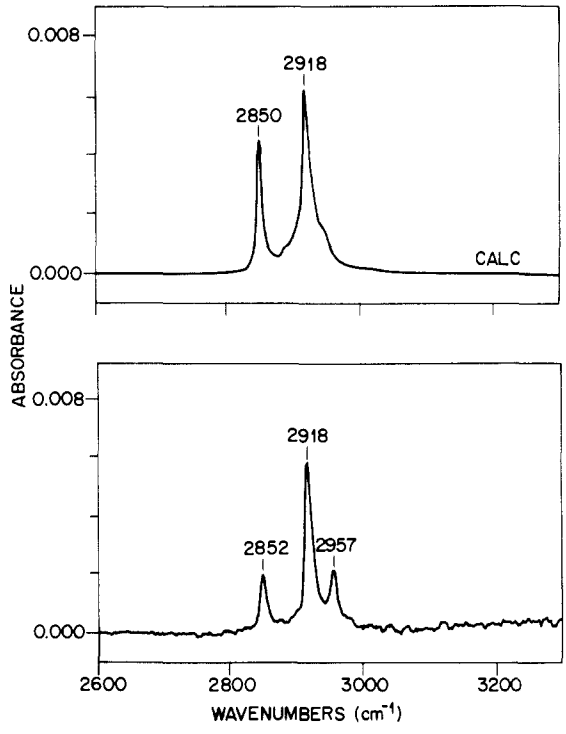

Figure 4. Calculated and experimental infrared reflection spectra for a methyl 16-mercaptohexadecanoate ($HS(CH_2)_{15}CO_2CH_3$) monolayer on gold in the high frequency region.

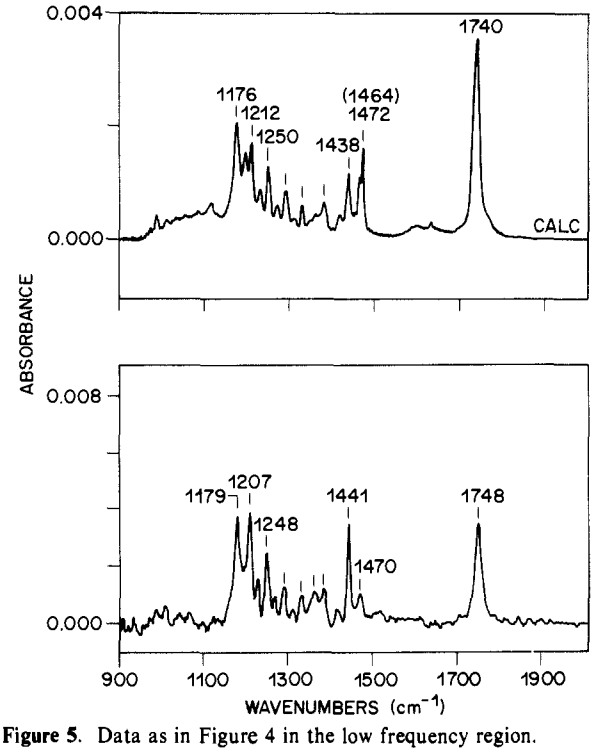

Figure 5. Data as in Figure 4 in the low frequency region.

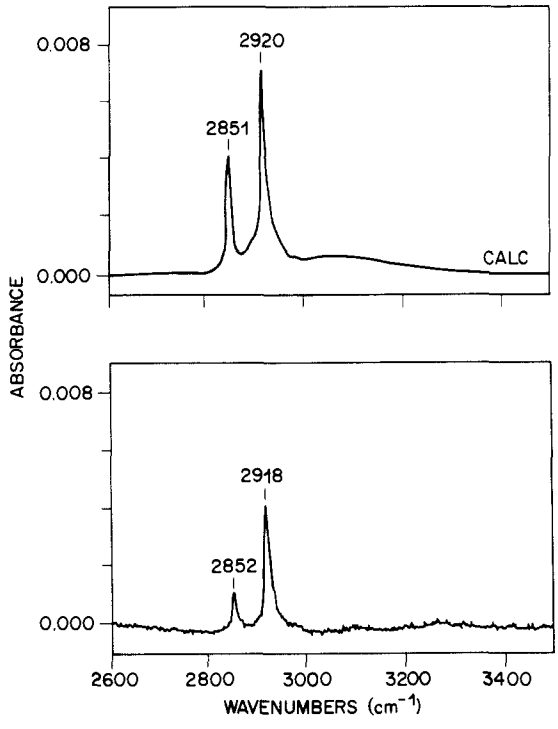

Figure 6. Calculated and experimental infrared reflection spectra for a 16-mercaptohexadecanoic acid ($HS(CH_2)_{15}CO_2H$) monolayer on gold in the high frequency region.

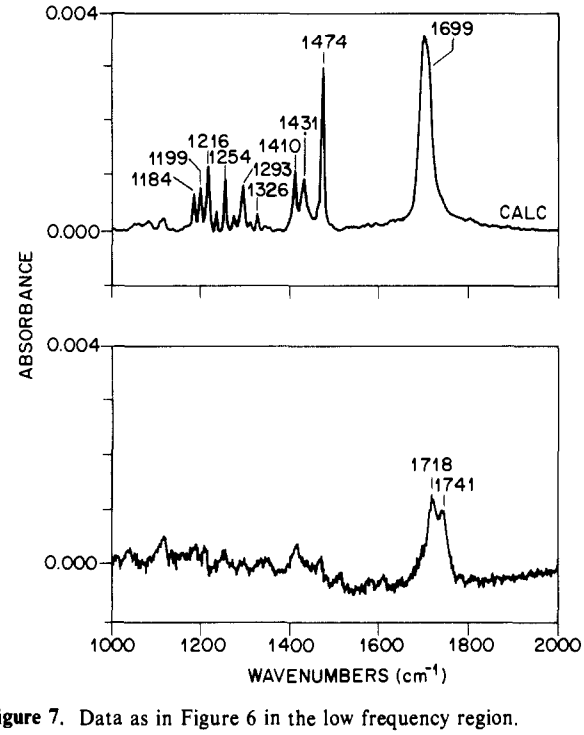

Figure 7. Data as in Figure 6 in the low frequency region.

rotation (β) around the chain axis of ~55° as shown in Figure 12. As was the case before, the sign of α cannot be determined from these data alone. It should be noted that the *range of chain cants described* (from the high of 40° to the low of 28°) *are well within the estimated total error limits of this analysis*, and any trends should be interpreted cautiously with regard to establishing subtle variations of structure. While such correlations probably do exist, they should be confirmed rigorously by independent techniques.

(C) Substituted Alkanethiols: Low-Frequency Modes. Examination of the lower frequency portion of the spectra (Figures 5, 7, 9, and 11) shows a variety of detailed information specific to each monolayer. The spectrum of the methyl ester derivative contains the richest detail and will be discussed first.

The methyl ester spectrum (Figure 5) has two prominent, easily interpreted features. First, a series of sharp bands between ~1200 and 1350 cm^{-1} is clearly seen in both the observed and calculated spectra; these absorptions have nearly identical positions and relative intensities. These bands are assigned to the progression of CH_2 twisting and wagging modes. The fact that they are strong compels the conclusion that the polymethylene chains exist in all-trans zigzag conformations with few if any gauche defects. These so-called progression bands are expected, of course, in the calculated spectrum *since it is based on a crystalline reference state* consisting of all-trans chains. Their presence and intensity

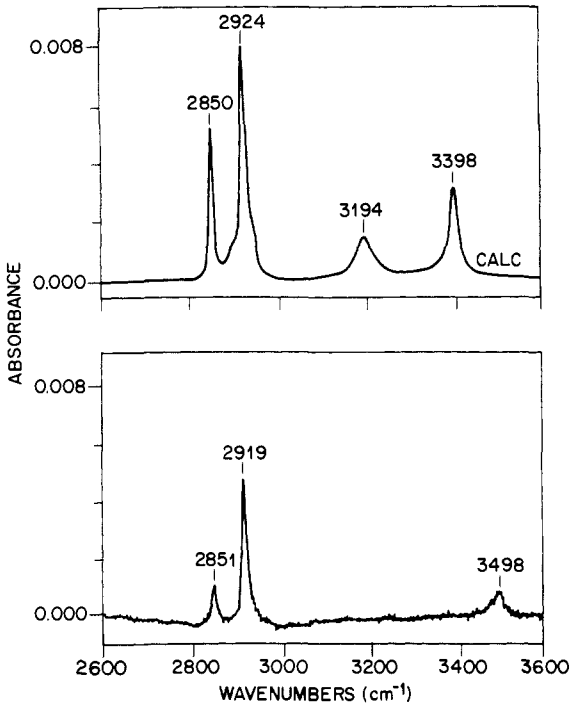

Figure 8. Calculated and experimental infrared reflection spectra for a 16-mercaptohexadecanamide ($HS(CH_2)_{15}CONH_2$) monolayer on gold in the high frequency region.

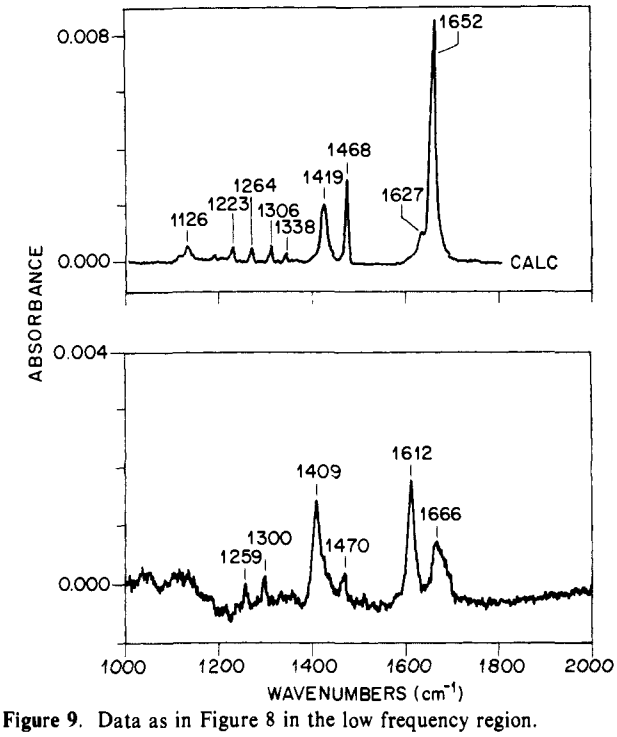

Figure 9. Data as in Figure 8 in the low frequency region.

in the monolayer spectrum, together with the results for the CH_2 C–H stretching modes presented above, strongly support a structure of the monolayer consisting of densely packed, crystalline assemblies of alkyl chains. These data by themselves, however, do not directly establish periodic chain–chain arrangements (such as a diffraction experiment would). Since the dispersed mode absorptions differ between the observed and calculated states only in their intensities, one can assign from them the orientation of the chains with respect to the surface. In order to do this properly, the individual bands for these modes must be specifically identified and a transition moment direction assigned. The observed spectra are actually a mixture of CH_2 wagging vibrations appearing in the same region as complex twisting and rocking modes.[20] We have examined the three most intense features (1248, 1288, and

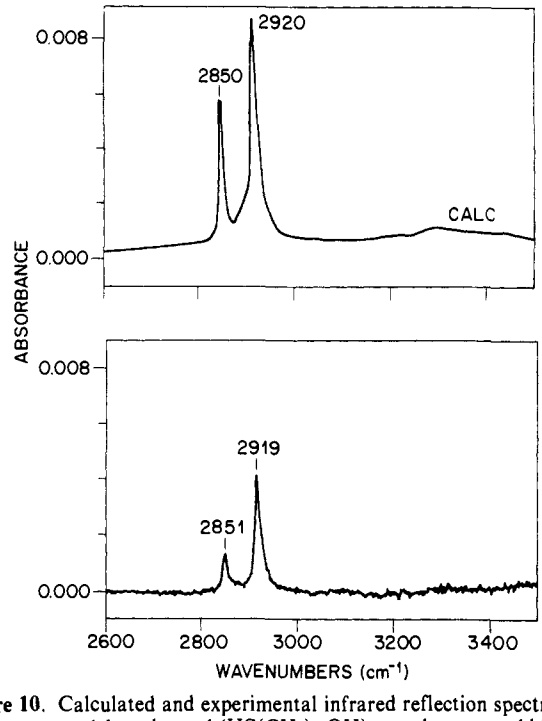

Figure 10. Calculated and experimental infrared reflection spectra for a 16-mercapto-1-hexadecanol ($HS(CH_2)_{16}OH$) monolayer on gold in the high frequency region.

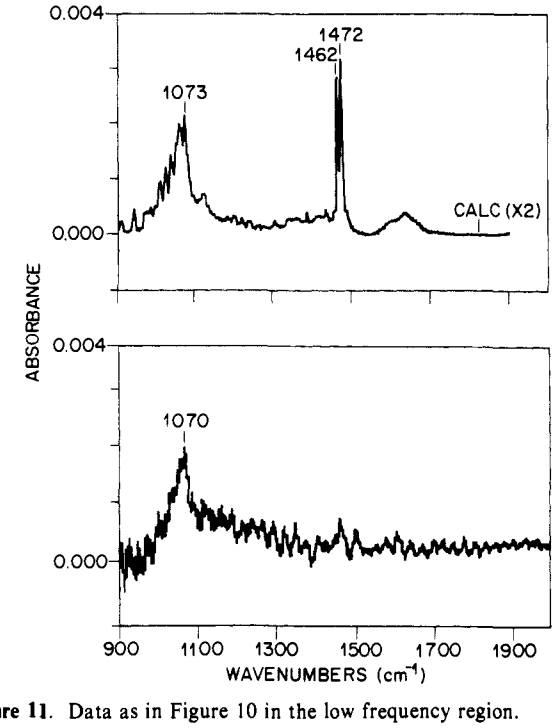

Figure 11. Data as in Figure 10 in the low frequency region.

1331 cm^{-1}) and assigned them to wagging vibrations with odd integral values of the phase state.[20] These modes exhibit transition dipoles parallel to the chain axis.[22] On this basis, the chain tilt angles are given directly by the θ_{mz} values (31, 35, and 40°); the average value obtained is 36°. The chain tilt estimated from the CH_2 stretching modes of the ester derivative is 38° (Table VII) and is in very good agreement with this average value.

Another obvious spectral feature is the strong band appearing at 1740 and 1748 cm^{-1} in the calculated and observed spectra, respectively. This band is assigned to the C=O stretching mode. It is notable that the peak frequency is 8 cm^{-1} higher in the monolayer spectrum. This result is not without precedent as we have observed similar frequency shifts in other monolayer systems

(22) Snyder, R. G. *J. Mol. Spectrosc.* **1960**, *4*, 411–434.

Table II. Spectral Mode Assignments and Calculated Transition Moment Directions for Methyl 16-Mercaptohexadecanoate on Au

freq, cm^{-1} obs	freq, cm^{-1} calc[b]	mode assignment[a]	$I_{obs}/3I_{calc}$	θ_{mz}, deg
2957		CH_3 C–H str (asym, op)	*c*	
2918	2918	CH_2 C–H str (asym), d^-	0.25[d]	60
2852	2850	CH_2 C–H str (sym), d^+	0.12	70
1748	1740	C=O str	0.28	58
1470	1472, 1464[e]	CH_2 scissors def, δ	0.19	65
1441	1438	CH_3O CH_3 bend (sym)[f]	0.94	14
~1200–1350	~1200–1350[g]	chain wags and twists[h]	*i*	36
1207	1212 (1196)	C–O str		
1179	1176	C–O str	0.69	34

[a] See footnote *a*, Table I. [b] Details given in text. [c] Quantitative analysis of this absorption was not attempted because of the poor resolution in the calculated spectrum caused by overlap with adjoining absorptions, particularly the d^- and CH_3 sym str (FR) modes. [d] Quantitative analysis of this absorption is complicated because of overlap with adjoining CH_3 modes. [e] Band split by crystal field interactions. [f] This band is assigned in analogy with that for CH_3OCOCH_3 (see: Wilmhurst, J. K. *J. Mol. Spectrosc.* **1957**, *1*, 201–215). This suggests that the asymmetric mode could appear near 1469 cm^{-1} where the CH_2 bend occurs. This contribution would lower the presumed CH_2 bend intensity and raise θ_{mz} above 65°. [g] Peaks assigned to this series are, observed, 1207, 1227, 1248, 1269, 1288, 1312, and 1331 cm^{-1} and, calculated, 1212, 1231, 1250, 1272, 1291, 1312 and 1330. The bands at 1207 (obs), 1212 (calc), 1248 (obs), and 1250 (calc) cm^{-1} could also contain contributions from C–O vibrations (ref 19). [h] See footnote *d* in Table I. [i] The strongest and best resolved bands in the series were used: 1248, 1250; 1288, 1291; 1331, 1330; the values of $I_{obs}/3I_{calc}$ are 0.73, 0.58, and 0.67, respectively, and the corresponding angles are 31°, 40°, and 35°. Since these peaks are not free of overlap with adjacent peaks, the calculated values should be considered as approximate. These bands were assigned as members of the wagging series with values of 3, 5, and 7 for the eigenstate indices (see footnote e, Table I).

for terminal groups exposed at an ambient interface.[4,13] This apparently general phenomenon seems to indicate that a correlation exists between bond stretching frequency and changes in the number (and perhaps polarizability and geometric arrangement) of neighboring atoms and/or groups. One extreme limit of this type of phenomenon is the generally observed decrease in frequency for many vibrations when an oscillator is taken from a gas-phase to a condensed-phase environment.

With respect to the C=O absorption, a calculation of the average transition moment direction from the spectral intensity (Table II) gives a value of ~58° from the normal to the surface. Further information regarding the headgroup orientation can be obtained from a calculation of the θ_{mz} value of the C–O stretch. The result we obtain (Table II) is 34°. Both these values, however, must be considered *very approximate* in as much as the transition moment directions are not expected to be directly along these bond axes.[19,23] The relatively strong absorption at 1441 and 1438 cm^{-1} in the observed and calculated spectra, respectively, can be assigned to the CH_3 symmetric bending mode (Table II) of the OCH_3 group. The value of θ_{mz} is 14° (Table II), and the transition moment is estimated to be parallel to the O–CH_3 bond. This suggests that the O–CH_3 bond is pointing close to perpendicular to the surface.

An estimation can be made of the surface geometry of the terminal ester group by adjusting the orientation of a model structure and looking for the best fit to the θ_{mz} values for the various modes associated with this group. A schematic representation of the terminal group geometry is shown in Figure 14. The best fit model orientation derived from *all* the observed θ_{mz} values (Table II) gives a chain cant $\alpha = -38°$ (in the opposite direction as that established for the alkanethiol monolayers). If the chain were canted in the same direction as that found for these latter monolayers, a very good fit could be obtained to the θ_{mz} values for the C=O stretching and OCH_3 methyl symmetric bending absorptions. In this analysis, the C=O bond would project upward at an angle of 32° from the surface plane; the O–CH_3 bond would lie very nearly along (~14° off) the surface normal. Perhaps the most attractive feature of this model is that the value of $\psi_{C\text{-}CO_2}$ (~40°) would be close to the |45°| value derived intuitively from the consideration of space-filling models. There would have to be, however, a large error (~30–40°) associated with the assignment of the carbonyl C–O (single) bond orientation. Considering all the evidence and given the uncertainty surrounding C–O transition dipole direction, we believe that this latter interpretation is in fact correct. This model also preserves a common and chemically reasonably geometry for the Au–S bond (see above).

The spectrum of the acid monolayer in the lower frequency region (Figure 7) shows features too weak relative to the noise to allow detailed interpretation except for the doublet of peaks at 1718 and 1741 cm^{-1}. Assignment of the doublet to C=O stretching mode absorptions is straightforward, but further interpretation with regard to specific structures is not.

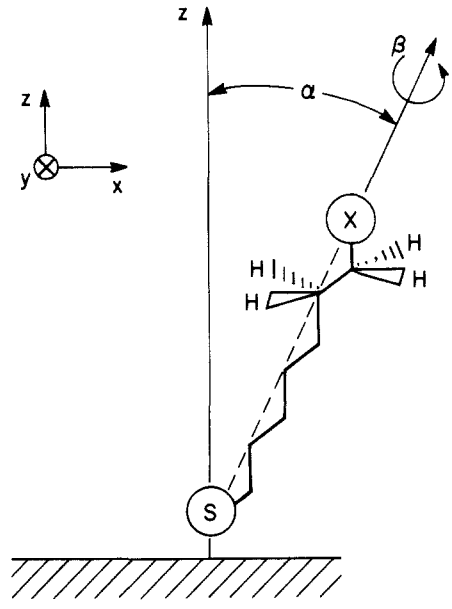

Figure 12. Tilting and rotation of an all-trans alkyl chain in surface coordinates. The initial configuration of the chain is with the main axis parallel to *Z* and the CCC plane parallel to the *X*, *Z* plane. The tilt and rotation angles are α and β, respectively.

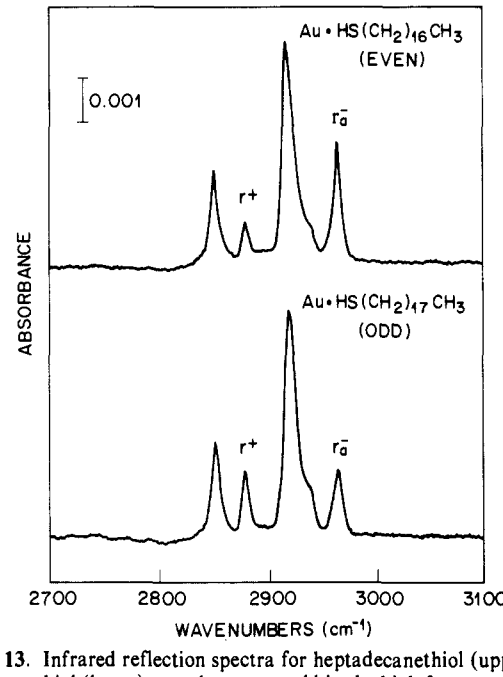

Figure 13. Infrared reflection spectra for heptadecanethiol (upper) and octadecanethiol (lower) monolayers on gold in the high frequency region. Mode assignments and interpretations are discussed in the text.

(23) Boerio, F. J.; Bahl, S. K. *Spectrochim. Acta* **1976**, *32A*, 987–1006. Popov, E. M.; Kogan, G. A.; Struchkova, M. I.; Zheltova, V. N. *J. Struct. Chem.* **1972**, *12*, 49–54.

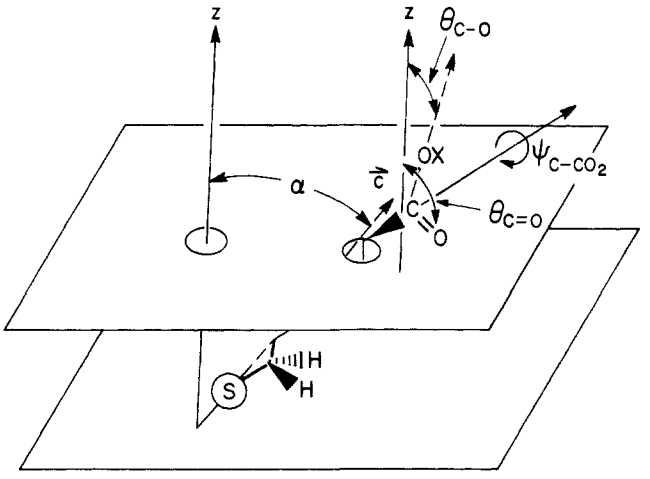

Figure 14. Schematic representation of a tilted chain on a surface showing the parameters defining the geometry of a terminal carbonyl group derivative. The orientation of this group is discussed in the text.

It seems reasonable to infer that the orientation of the carbonyl in the terminal CO_2H group might be similar to that of the methyl ester (refer to Figure 14 and the previous discussion). The average value of θ_{mz} we derive for the two C=O groups (given the assumptions described in Table III) is 66° which is similar to that of the ester (58°). This orientation would leave the O–H group exposed at the surface. It is well-known that carboxylic acids undergo strong intermolecular hydrogen-bonding interactions, particularly in condensed phases.[24-26] The calculated spectrum (based on the polycrystalline parent compound) shows a peak at 1699 cm^{-1} (Figure 7) which is consistent with a hydrogen-bonded dimer structure.[26] In the present case of the monolayer, however, the formation of head-to-head dimers is clearly impossible. It seems more likely that linear polymeric chains of hydrogen bonds could arise by alignment of sequences of neighboring CO_2H groups in the surface plane. Such chains are commonly observed for crystalline acids of low molecular weight.[27,28] In the present case we believe that the 1718-cm^{-1} absorption is due to the hydrogen bonded C=O groups of such a chain structure, while the 1741-cm^{-1} absorption represents non-hydrogen-bonded (or weakly bonded) groups. If one assumes that the surface phase present consists of similar orientations and that the absorption cross sections for both the groups are roughly equal, the observed absorption intensities (Figure 7) imply only two CO_2H groups per interaction sequence. The hydrogen bonding interactions in these dimers (or short sequences) also appear to be somewhat weaker than that which occurs in linear acetic acid chains.[27,28] We emphasize here that the understanding of structural effects in hydrogen bonding of carboxylic acids is not well-developed so any discussions of structural details are, at best, suggestive.

The low frequency spectrum of the amide derivative is shown in Figure 9. A number of interesting features are apparent in the data which distinguish the molecular environment in the monolayer. The calculated spectrum shows a strong band at 1652 cm^{-1} and a barely resolved, weak band at 1627 cm^{-1}. These are assigned as the typical amide I and II bands which are attributed to modes approximately described as C=O stretching and N–H bending.[19,29] In the monolayer, considerable changes in the molecular environment are evident as judged by the appearance in this region of a very asymmetric shaped band at 1666 cm^{-1} and another band at 1612 cm^{-1}. Comparison of calculated and monolayer spectra suggest significant restructing of the amide group in the monolayer relative to the bulk crystalline state, in particular, the increased splitting of the amide I and II bands into a higher and a lower frequency component and the significant redistribution of intensity. Because of the additional complexities of amide hydrogen-bonding interactions relative to the simpler case of CO_2H groups (see above), we cannot interpret these spectral changes in terms of specific structures with any confidence. The only other low frequency features we discuss here are the 1468, 1470 cm^{-1} bands which we attribute to the CH_2 scissors deformation in the calculated and monolayer spectra, respectively. The direction of the transition moment calculated from the δ_{CH_2} spectral intensities in Figure 9 is 71° (see Table IV). With use of the molecular coordinate direction in Table VI, a value of 32° is calculated for the chain tilt angle (Table VII) with a rotation around the chain axis of 55°. These values are in good agreement with the values determined from the C–H stretching mode absorption data (Table VII).

The lower frequency spectrum of the alcohol is shown in Figure 11. Due to the weakness of the spectrum relative to the noise, only qualitative conclusions can be made about the environment of the hydroxyl group in the alcohol surface. We assign the bands at ~1070 (monolayer) and 1073 cm^{-1} (calculated) to the C–O stretch. By using eq 3, we estimate that the angle of the C–O bond with respect to the surface normal is about 50°. As shown in Table VII, this value fits reasonably well with a model chain having the CCO bonds coplanar with the CCC chain and the C–OH group at an angle of ~40° from the surface (Figure 12 for X = CH_2OH).

The series of bands appearing at the low frequency side of the 1073-cm^{-1} peak are attributed to a complex series of CH_2 rocking and twisting modes, indicating an all-trans conformational sequence in the crystalline reference state. These bands appear to be slightly resolved in the monolayer spectrum; no attempt was made to calculate a chain tilt angle from them.

Table III. Spectral Mode Assignments and Calculated Transition Moment Directions for 16-Mercaptohexadecanoic Acid on Au

freq, cm^{-1}				
obs	calc[b]	mode assignment[a]	$I_{obs}/3I_{calc}$	θ_{mz}, deg
	~3050	O–H str		
2918	2920	C–H str (asym), d^-	0.196	64
2852	2851	C–H str (sym), d^+	0.096	72
1741				
1718	1699	C=O str	0.17[c]	66
1471 (?)	1474	CH_2 scissors def, δ	≲0.09[d]	≳73
	1431	C–O str[e] (+ ip COH bend)		
~1412 (?)	1410	α-CH_2 scissors def, δ_α[f]	*f*	
g	~1150–1350[g]	chain wags and twists	*h*	

[a] See footnote *a*, Table I. [b] Details given in text. [c] This value is determined by integrating the total absorption intensity of the bands. The interpretation of orientations from this data is considered qualitative because significant changes in the optical functions are expected to occur as a result of hydrogen-bonding interactions (for example, see: Coleman, M. M.; Lee, K. H.; Skrovanek, D. J.; Painter, P. C. *Macromolecules* **1986**, *19*, 2149–2157) and because multiple species (at least two distinct ones in the monolayer) are present (each of which can possess its own unique orientation). [d] Value calculated as an upper limit based on the assumption that the actual intensity of the monolayer CH_2 scissors mode can be no greater than the spectral feature selected at 1471 cm^{-1}. [e] This mode is thought to contain a substantial C–O–H bending character (ref 19, 26, and 28). [f] The CO_2H group adjacent to the α-CH_2 causes a shift in frequency and an increase in intensity relative to the internal CH_2 groups in the chain (ref 19). Quantitative treatment of the intensities were not done because of this effect and uncertainties caused by changes in the CO_2H environment (e.g., H-bonding). [g] Absorptions in the calculated spectrum which are assigned to this series appear at 1184, 1199, 1216, 1234, 1254, 1293, and 1326 cm^{-1}. The intensity pattern in the observed monolayer spectrum follows this sequence within ±2 cm^{-1} suggesting the appearance of these modes rather than random noise in the base line. [h] Quantitative interpretation of these modes was not made because of the uncertainty of their appearance in the monolayer spectrum (see footnote *g*) and the inability to observe line widths, relative intensities, and other pertinent features that one typically examines in this series.

(24) Kishida, S.; Nakamoto, K. *J. Chem. Phys.* **1964**, *41*, 1558–1562.
(25) Haurie, M.; Novak, A. *J. Chim. Phys. Phys.-Chim. Biol.* **1965**, *62*, 146–57.
(26) Umemura, J. *J. Chem. Phys.* **1978**, *68*, 42–8.
(27) Krause, P. F.; Katon, J. E.; Rogers, J. M.; Phillips, D. B. *Appl. Spectrosc.* **1977**, *31*, 110–15.
(28) Teragni, P.; Masetti, G.; Zerbi, G. *J. Chem. Phys.* **1978**, *28*, 55–72.
(29) Suzuki, I. *Bull. Chem. Soc. Jpn.* **1962**, *35*, 1279–86.

Table IV. Spectral Mode Assignments and Calculated Transition Moment Directions for 16-Mercaptohexadecanamide on Au

freq, cm^{-1} obs	freq, cm^{-1} calc[b]	mode assignment[a]	$I_{obs}/3I_{calc}$	θ_{mz}, deg
3498		N–H str (free)[c]		
	3398	NH str (H-bonded, asym)[d]		
	3194	NH str (H-bonded, sym)[d]		
2919	2924	C–H str (asym), d^-	0.18	65
2851	2850	C–H str (sym), d^+	0.079	74
1666	1652	C=O str[e]	0.0072[h]	85
1612	1627	NH_2 bend[f]	0.57[h]	41
1470	1468	CH_2 scissors def	0.12	71
1409	1419	C–N str[g]	0.25[i]	60
1300		*j*		
1259		*j*		
	~1100–1350	chain wags and twists[j]	*k*	

[a] See footnote *a*, Table I. [b] Details given in text. [c] This peak is probably the antisymmetric stretching mode of the N–H stretch of the free NH_2 group. The antisymmetric mode typically appears at ~3520 cm^{-1} and the symmetric at ~3410 cm^{-1} for free NH_2 (ref 19). [d] These frequencies fit the general pattern for alkylamides in the solid state (ref 19 and Dollish, F. R.; Fateley, W. G.; Bentley, F. F. *Characteristic Raman Frequencies of Organic Compounds*; J. Wiley: New York, 1974). [e] This corresponds to the amide I band (see ref 19). [f] This corresponds to the amide II band (see ref 19). [g] See ref 29. [h] Quantitative interpretations of these band intensities are of uncertain reliability because of the effects of hydrogen bonding on the modes. [i] The calculation is based on the 1409-cm^{-1} band in monolayer with the assumption of a symmetrical band shape with the same half width as the 1419-cm^{-1} band in the calculated spectrum. The broad high frequency tail in the monolayer band could be due to strongly hydrogen-bonded NH_2 groups. A distribution of hydrogen-bonded species is suggested by the asymmetric shape of the amide I band (1666 cm^{-1}) (see footnote *e* also). [j] Bands assigned to this series appear at 1223, 1264, and 1306 cm^{-1} in the reference (calculated) spectrum. Other members at lower intensities can also be observed but are not given here. The bands at 1259 and 1300 cm^{-1} in the monolayer spectrum appear to be members of this series, but if so one must explain why the member corresponding to 1223 cm^{-1} in the reference spectrum is missing. The latter could be due to some negative artifact (reference contamination is a typical source) suggested in the monolayer spectrum base line noise pattern at ~1220 cm^{-1}. [k] Calculations were not done with these modes because of uncertainties in the appearance of all the bands in the monolayer spectrum (see footnote *j* above).

Table V. Spectral Mode Assignments and Calculated Transition Moment Directions for 16-Mercaptohexadecanol on Au

freq, cm^{-1} obs	freq, cm^{-1} calc[b]	mode assignment[a]	$I_{obs}/3I_{calc}$	θ_{mz}, deg
	~3300	O–H str (H-bonded)		
2919	2920	C–H str (asym), d^-	0.14	68
2851	2850	C–H str (sym), d^+	0.076	74
	1472	CH_2 scissors def,[c] δ	$\lesssim$0.11[d]	$\gtrsim$71
	1462			
1070	1073	C–O str	0.41	50
	950–1070	chain rocking[e]	*f*	*f*

[a] See footnote *a*, Table I. [b] Details given in text. [c] The splitting observed in the KBr matrix-based spectrum is caused by crystal field interactions in the unit cell. [d] A limit was estimated by examining the feature in the observed spectrum at ~1466 cm^{-1} and measuring its (area) intensity. Since this feature may be noise, this calculation then sets an upper limit on I_{obs}. [e] The series of sharp bands on the low frequency side of the ~1073-cm^{-1} band is attributed to a complex dispersion of rocking and twisting modes of the chain CH_2 groups (see ref 22). The bands occur at 974, 984, 996, 1008, 1022, 1037, 1051, and 1063 cm^{-1}. [f] Any chain mode absorption in the observed spectrum is barely observable above the noise. In addition, no assignments of bands could be made to individual phase values and corresponding transition moment directions.

Determination of the Strength of Intermolecular Interactions Using Temperature-Programmed Desorption. The infrared data discussed above strongly suggest that the environment of the hydrocarbon chains is similar to that experienced in a hydrocarbon crystal. To more completely develop this point and to answer the question of how the interaction of these chains contributes to the stability of the monolayer phases, we have made a preliminary examination of thermal stability by using temperature-programmed desorption (TPD). Figure 15 shows a TPD trace for the desorption of a hexadecanethiol monolayers from an Au(111) single-crystal surface. This spectrum was interpreted for convenience according to the standard method described by Redhead[30] *assuming first-order desorption* and a preexponential factor of 1×10^{13} s^{-1}.[31] With these assumptions, we calculate that the activation energy for a *hypothetical* molecular desorption process is ~40 kcal/mol.[32] Similar values are obtained from analyses of TPD data from the acid- and amide-terminated monolayers.

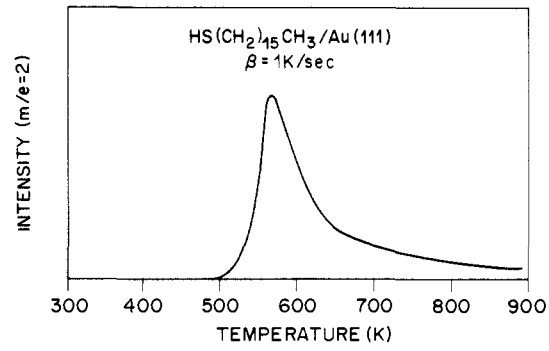

Figure 15. Temperature-programmed desorption (TPD) data for a hexadecanethiol monolayer chemisorbed on an Au(111) single-crystal surface. The temperature ramp rate used was 1.0 K/s. The intensity of the $m/e = 2$ ion was followed. Similar desorption spectra are seen for the other thiols as well.

To arrive at a proper understanding of this result, qualitative though it may be, we need to consider the earlier work from our laboratory which describes the nature of the interactions of simple organosulfur compounds on Au(111).[3] A strongly bound state was identified by using dimethyl disulfide as the adsorbate. (There is considerable evidence which suggests that in solution adsorption experiments both thiols and disulfides enter the same strongly chemisorbed state, a surface thiolate, on Au(111); in the reported UHV experiments, only the disulfide accessed this state due to the kinetic limitations of the experiment.) The data showed that, at saturation coverage, the heat of adsorption of the thiolate is ~28 kcal/mol. Desorption was a clean process yielding dimethyl disulfide. Since the lateral interactions of methyl groups are not likely to contribute much to the observed stability of this monolayer, it is reasonable to attribute the bulk of the effect to the interaction of the gold surface with the sulfur atom. The enhanced stability of the *n*-C_{16} monolayer, then, must reflect the contribution of the now significant lateral interactions of the alkyl chains. This implies a stabilization of the monolayer of ~0.8 kcal/mol of CH_2 groups. This value is slightly larger than either the group constituent heats of fusion or vaporization of a normal paraffin (~0.6 kcal/mol of CH_2)[33] and less than the van der Waal's interaction energy of crystalline hydrocarbon chains.[34] It is also suggestive of an interaction which is stronger than that which characterizes hydrocarbon liquids, a notion consistent with the IR data above. It is our belief, however, that the 0.8 kcal/mol figure is merely an estimate of the *lower limit* of the hydrocarbon interaction energy in this system, as the desorption process is not the same for the two adsorbates. This is most clearly shown by AES analysis of the gold surface after the desorption of the C_{16} monolayer. We observe both carbon and sulfur indicating that the desorption

(30) Redhead, P. A. *Vacuum* **1962**, *12*, 203–11.
(31) This is equivalent to the assumption that $\Delta S^* \simeq 0$.
(32) We have followed the intensity of $m/e = 2$ in this experiment (H_2^+) as this ion is produced both as an ionization cracking fragment of any potential hydrocarbon species desorbed from the surface as well as from an H_2 coproduct. This ion is thus suitable for detecting (though not identifying or quantifying) a molecular desorbing species as well as a decomposition product.
(33) Estimated from literature values; *CRC Handbook of Chemistry and Physics*, 53rd ed.; CRC Press: Cleveland, OH, 1973.
(34) The reported value is ~1.8 kcal/mol of CH_2 at 0K; The value of interest at the higher temperature here is likely to be at least 0.5 kcal/mol less than this: See: Salem, L. *J. Chem. Phys.* **1962**, *37*, 2100–2113.

Table VI. Selected Transition Moment Directions in Molecular Coordinates[a]

compd	mode	estimated direction of M in molecular coordinates[b]
$HS(CH_2)_{15}CO_2H$	>C=O str	∥ C=O bond
all	CH_2 CH str (asym)	ip HCH, ∥ to axis through H atoms
	CH_2 CH str (sym)	ip HCH, bisect HCH
	CH_2 scissors def	ip HCH, bisect HCH
	$-(CH_2)-$wags[c]	∥ to all trans chain axis
$HS(CH_2)_{15}COOCH_3$	CH_3 C-H str (sym)	∥ O-CH_3 bond
	CH_3 C-H str (asym)	⊥ O-CH_3 bond[d]
	>C=O str	∥ to C=O bond
	$-CO-OCH_3$, C-O str	*e*
	$-COO-CH_3$ C-O str	*e*
$HS(CH_2)_{16}OH$	C-O str	∥ to C-O bond
$HS(CH_2)_{15}CONH_2$	C=O str	∥ to C=O bond
	N-H bend	*f*
$HS(CH_2)_{15}CH_3$	CH_3 C-H str (sym), r^+	∥ C-CH_3 bond
	CH_3 C-H str (asym), r_a^-	⊥ C-CH_3 bond, ip CC backbone
	CH_3 C-H str (asym), r_b^-	⊥ CC backbone plane, op
	CH_3 def (sym)	∥ C-CH_3 bond

[a] Directions are approximated from the normal mode descriptions. Exact directions could be several degrees off those calculated from the normal mode potential energy distributions and need to be determined from charge distribution calculations. [b] Symbols used: ∥ = parallel, ⊥ = perpendicular, ip = in plane, op = out of plane. [c] This assignment is made specifically for a $(CH_2)_{15}$ polymethylene chain and for odd members of the wagging series. Details are given in footnotes *d* and *e* in Table I. [d] There should be two spatially degenerate modes for this vibration. For this ester group the directions are not known although one might presume for a fixed ester conformation the modes are in and out of the COC plane. No assignment of a direction of the 2957-cm^{-1} band other than that given in the table is made here. [e] Approximated by the direction of the C-O bond. However, this mode contains contributions from C=O stretching and other motions of the ester group (see ref 19 and 23). [f] The direction of this transition moment is probably affected by hydrogen bonding but for the sym bending should be nearly parallel to the C-N bond (for a planar-trigonal N) (see ref 29).

product is no longer exclusively disulfide as was the case for the methylthiolate surface species. This desorption process, occurring as it does at a higher temperature, is accompanied by extensive decomposition of the adsorbate. It thus seems reasonable to infer that a desorption process yielding dialkyl disulfide (one mechanistically related to the methylthiolate desorption discussed above) must be more highly activated than this decomposition pathway. It should also be noted that the assumption that the preexponential term is $\sim 1 \times 10^{-13}$ s^{-1} is a poor one. It is likely that a proper value would be larger and that the true enthalpy of activation is several kcal/mol higher. This would serve to increase the 0.8 kcal/mol number cited above.[35,36]

The Unique Molecular Environment Experienced by the Chain-End Groups. The analyses given above suggest that common features characterize the polymethylene chains in a diverse series of monolayers. We are thus led to wonder, can general conclusions also be reached as regards the characteristics of the chain-terminating functionality in these materials? It is obvious from the data that the chain-end groups exist in environments atypical of most organic materials. It is clear that no simple reference state such as bulk solids or gases provide accurate models with regard to detailed vibrational states and optical functions. We will now consider this aspect in detail from the point of view of defining some specific issues. Detailed physical models of these phenomena will not be presented in this paper.

One interesting aspect is the spectral perturbation of the methyl groups in the alkanethiol monolayers. These groups should experience relatively simple interactions at the interface since no significant hydrogen-bonding interactions are possible. However, as was pointed out earlier in this paper, both the C-H stretching and the symmetric bending vibrations of the methyl group exhibit abnormalities within our method of analysis. We discuss each in turn. The three C-H stretching modes (sym, asym ip, and asym op; refer to Table I) have mutually orthogonal transition moments (see Table VI). As a result, one would expect for any given orientation of the CH_3 group to a chosen axis *z*, that the sum of $\cos^2 \theta_{mz}$ would be unity. The values in Table I, however, clearly exceed 1.0 by a significant amount (even exceeding 2.0 using the sym str at 2872 cm^{-1}). A similar observation was noted in an earlier paper which described the structure of a monolayer of hexadecyl disulfide on gold.[4] A comparable failure of the model is also found to occur with an analysis of the symmetric deformation mode (1372 cm^{-1}; Table I). The intensity of this absorption is so much greater in the monolayer compared to the calculated spectrum that $\cos^2 \theta_{mz}$ determined from eq 3 would greatly exceed unity. The physical untenability of these calculations must arise from the fact that *other factors besides orientation enter into the differences between the crystalline reference state and the monolayer.* The actual values of the optical functions (related to the polarizability and transition moment of the oscillator in a local environment), thus, must be significantly different for the crystalline solid and the interface. This problem is compounded further as a result of the strong Fermi resonance and its effect on the C-H stretching modes. The correlation between the dynamic charge distributions of the CH_3 group and the interface structure are not clear but several experiments suggest that simple (but presently not understood) dielectric effects may be important.[37] In these experiments, thin organic overlayers were placed over a hexadecanethiol monolayer. The spectra of the CH_3 group in the C-H stretching region showed that, in these environments, a significant reduction in intensity of the r_a^- (ip) mode occurs.[38] Further

(35) Whitesides and co-workers, by measuring the desorption of thiol monolayers isothermally in solution, found a chain length dependence of the activation energy of 0.2 kcal/mol of CH_2.[5] While this value cannot be compared in a simple, unambiguous manner to tht given here, it does suggest that the interaction energy is greater than that of a simple hydrocarbon liquid.

(36) Given the constrained nature of the adsorbate in this dense monolayer phase, the preexponential term is likely to be closer to 10^{16} s^{-1}. This would change the measured barrier by ~5 kcal/mol. Analysis of the leading edge of ihe TPD trace in Figure 14 using a "differential" technique (Habenschaden, E.; Küppers, J. *Surf. Sci.* **1984**, *138*, L147–L150) yields an activation energy of desorption of ~46 kcal/mol. The interaction energy suggested by these values increases to ~1.1 kcal/mol of CH_2 groups.

(37) Allara, D. L.; Nuzzo, R. G.; Dubois, L. H. Unpublished results. Chidsey, C. E. D. Private communication.

(38) It is important to note explicitly that the spectral abnormalities described above will complicate other methods of analysis as well. In particular, other less rigorous analyses which rely solely on the measurement and interpretation of spectral intensity ratios are also likely to fail should the analysis be made by using a mode which is significantly perturbed by the interfacial environment. Indeed, *without the cross-check afforded by the quantitative treatment of discrete band intensities, such perturbations could go unnoticed.*

Table VII. Transition Moment Orientations from Spectral Intensities and Molecular Models of Tilted and Rotated Alkyl Chains

monolayer	mode[a] ($\bar{\nu}$, cm^{-1})	θ_{mz}, deg calc from		model chain orientation,[b] deg	
		spectra[c]	model[d]	α	β
$HS(CH_2)_{15}CH_3$				40	50
	r_a^- (2965)	25			
	r_b^- (2958 (sh))	~69			
	d^- (2919)	61	61		
	d^+ (2850)	65	66		
	δ_{CH_2} (1468)	66	66		
	wag-twist (1150–1350)	~39[e]	40		
$HS(CH_2)_{15}CO_2CH_3$				38	55
	d^- (2918)	60	60		
	d^+ (2852)	70	69		
	δ_{CH_2} (1470)	65			
	wag-twist (~1200–1350)	36	38		
$HS(CH_2)_{15}CO_2H$				32	55
	d^- (2918)	64	64		
	d^+ (2852)	72	72		
	δ_{CH_2} (1471)[f]	≳73	72		
$HS(CH_2)_{15}CONH_2$				31	55
	d^- (2919)	65	65		
	d^+ (2851)	74	74		
	δ_{CH_2} (1470)	71	74		
$HS(CH_2)_{15}CH_2OH$				28	50
	d^- (2919)	68	67		
	d^+ (2851)	74	74		
	δ_{CH_2} (~1466)	≳71	74		
	C–O str (1070)	50	57[g]		

[a] See Tables I–V. Frequency given is for the observed monolayer spectrum. [b] Cant and twist angles of an all-trans zigzag chain (see Figure 12) which provides the best fit to experimentally determined values of θ_{mz}. Only the absolute value of α ($|\alpha|$) can be determined from CH_2 modes since the z components of their transition dipole moments are symmetrical with respect to the tilting operation. Arguments concerning the assignment of the absolute sign of α are presented in the text. [c] Data taken from Tables I–V. Details given in text. [d] Model shown in Figure 14. Values are those calculated from the model chain orientation (see footnote *b*). [e] See footnote *e*, Table I. [f] See footnote *d*, Table III. [g] In this model, the C–O bond is trans to the adjacent CH_2–CH_2 bond. Note that for this particular compound with a $(CH_2)_{15}$ chain, the group X in Figure 12 is a CH_2OH group.

experiments along these lines are in progress and will be reported elsewhere.

There are also other spectral perturbations we have observed that have strong bearing on the analysis of film structure. As has been discussed above, the complex, directional character of hydrogen bonding is a significant challenge to theoretical treatment. An additional example of a spectrally complex system was evidenced by a peculiarly varying character of the C–H stretching region for the alcohol monolayer system. In some samples we noted the appearance of a broad feature at ~2880 cm^{-1}. It is important to note that such samples had very low (<10°) contact angles with water and the ellipsometrically determined thickness was unchanged; from this we conclude that the feature is not an adventitious methyl-containing adsorbate. This feature also is found to disappear when the alcohol surface is allowed to react with trifluoroacetic anhydride. We conclude that it represents an example of the well-documented perturbation of neighboring C–H stretching modes by heteroatoms (in this case, the CH_2 adjacent to the OH group).[19] These effects, which are sensitive to molecular conformations, suggest some range of metastable conformations can exist at the chain tail for at least this one derivative. We believe a broader consideration of such structural complexities is warranted,[39] especially with regard to their importance in the presence of other contacting phases such as the liquids used in wetting studies.

Concluding Remarks

Chemisorption of ω-substituted normal chain thiols of the type described herein on gold surfaces of nominal (111) texture produces dense, highly oriented and perhaps ordered monolayer films by a self-assembly process. Variation of the chain-terminating functional groups—CH_3, CO_2H, $CONH_2$, CO_2CH_3, CH_2OH, and presumably others—has relatively little effect on the structure of the film in the region of the hydrocarbon chains. For the adsorbates studied, the chains adopt an all-trans zigzag conformation[40] and bond to the surface in a structure in which their main axis is canted ~34° from the normal.[41] The chains are also observed to twist their axis approximately 55° from a configuration with the CCC plane perpendicular to the surface plane. The spectral evidence suggest specific orientations for the functional groups at the ambient interface. The lateral density of these groups is high, suggesting that steric screening effects may play an important role in wetting and reactivity patterns. These groups, as evidenced by vibrational data, reside in chemically and physically distinct environments which are poorly modeled by bulk phases.

Future papers will detail studies which employ these well-defined model organic surfaces to explore the microscopic characteristics of wetting[12b] and interfacial reactivity.

Acknowledgment. We express our appreciation to Professor George M. Whitesides and his co-workers, especially Drs. Colin Bain, Lou Strong, and E. Barry Troughton, for many enlightening and helpful conversations. We are also grateful to our colleague Chris Chidsey for providing critical insights.

(39) Recent molecular dynamics calculations and X-ray diffraction studies strongly suggest that gauche conformations accumulate at the chain termina in related monolayer assemblies. See: Barton, S. W.; Thomas, B. N.; Flom, E. B.; Rice, S. A.; Lin, B.; Peng, J. B.; Ketterson, J. B.; Dutta, P. *J. Chem. Phys.* **1988**, *89*, 2257–70. Harris, J.; Rice, S. W. *J. Chem. Phys.* **1988**, *89*, 5898–908.

(40) The finding of an all-trans geometry of the chains in these films is further supported by the results of recent IR–visible SUM spectroscopy studies. See: Harris, A. L.; Chidsey, C. E. D.; Levinos, N. J.; Loiacono, D. N. *Chem. Phys. Lett.* **1987**, *141*, 350–56.

(41) Theory lends support to the structural trends developed in this paper in that chain tilts of this general magnitude are predicted by both simple two-dimensional lattice models (Outka, D. A.; Stöhr, J.; Rabe, J. P.; Swalen, J. D.; Rotermund, H. H. *Phys. Rev. Lett.* **1987**, *59*, 1321–24. Outka, D. A.; Stöhr, J.; Rabe, J. P.; Swalen, J. D. *J. Chem. Phys.* **1988**, *88*, 4076–87) and molecular dynamics calculations on closely related model systems (Cardini, G.; Bareman, J. P.; Klein, M. L. *Chem. Phys. Lett.* **1988**, *145*, 493–8. Bareman, J. P.; Cardini, G.; Klein, M. L. *Phys. Rev. Lett.* **1988**, *60*, 2152–55). These latter calculations suggest that the density of gauche defects is low.